https://doi.org/10.22645/udi.2023.06.30.001
도시과학 제12권 제1호 2023. 06. 1 - 10쪽

Effects of pre-curing periods on pore structures of ordinary Portland cement pastes with calcium silicate cement powder

Kim, Gwang Mok*

Abstract: The cement industry is a major source of carbon dioxide emissions. Reduction in emissions in this sector is an important issue. Calcium silicate cement is a type of alternative to ordinary Portland cements which contributes to the reduction in carbon dioxide emissions. However, because the type of cement is a non-hydraulic material, there are limitations to its application in the field. The effects of pre-curing periods on the physical characteristics of ordinary Portland cement pastes with calcium silicate cement in the present study were investigated. The Independent variable is the pre-curing period. The pre-curing period varied from 0 to 5 hrs, considering the hydration characteristics of ordinary Portland cement. The carbonation curing of the ordinary Portland cement pastes with the calcium silicate cement after pre-curing was conducted. The concentration of gaseous CO_2 was fixed at 20 %. The test results showed that the pre-curing period led to the pore structural change of the pastes, which in turn could affect the further reaction under the long-term curing condition.

Key Words: Carbon dioxide, Ordinary Portland cement, Calcium silicate cement, Pore structure, Carbonation curing

1. Introduction

The cement industry is one of the representative CO_2-emitting industrial sectors worldwide. The amount of CO_2 emitted from the cement industry is approximately 5% of global anthropogenic emissions, referring to the International Energy Agency (IEA) (Xu et al., 2014). The manufacturing process of ordinary Portland cement (OPC) such as the calcination of limestone and combustion of fuels for the synthesis of clinker in the kiln emits a large amount of CO_2. In particular, the calcination of limestone mostly induces CO_2 emissions in the cement industry.

Various efforts for the reduction in the CO_2 emission of the cement industry have been attempted such as the use of alternative fuels and supplementary materials, carbonation curing, and the development of alternative binders (Rahman et al., 2015; Zhang et al., 2017; Hasanbeigi et al., 2012; Juenger et al., 2011). Biomass and industrial wastes as alternative fuels have been employed to reduce the use of fossil fuels and improve energy efficiency (Rahman et al., 2015). Some industrial by-products such as coal ashes and blast furnace slag have been adopted to reduce the use of ordinary Portland cements and to improve the mechanical properties and durability of concretes (Hasanbeigi et al., 2012). Carbonation curing is one of the carbon capture and utilization (CCU) techniques. The technique is based on the carbon mineralization reaction that forms calcium carbonates and permanently sequestrates the CO_2 in a

* 한국지질자원연구원 자원활용연구본부 선임연구원, 교신저자 (k.gm@kigam.re.kr).

cementitious matrix as a form of mineral (Zhang et al., 2017). The application of alternative binders such as calcium sulfoaluminate (CSA) cements, alkali-activated cements, magnesia cements, and non-hydraulic calcium silicate cements (CSCs) have been investigated to reduce the use of OPC (Thomas et al., 2018; Provis, 2018; Walling and Provis, 2016; Wang et al., 2022). The aforementioned techniques directly and indirectly can contribute to the reduction in CO_2 emissions in the cement industry (Rahman et al., 2015; Zhang et al., 2017; Hasanbeigi et al., 2012; Wang et al., 2022).

Among these techniques, the use of CSCs is one of the most effective ways to reduce CO_2 emissions in the cement industry. Non-hydraulic CSCs consist of wollastonite ($CaO \cdot SiO_2$, CS), rankinite ($3CaO \cdot 2SiO2$, C_3S_2), and C_2S phases, while OPC includes a large amount of C_3S phase (Wang et al., 2022). That is, the content of limestone for the manufacture of the CSCs is lower than that of OPC (Wang et al., 2022). The calcination temperature for the manufacture of the CSCs is reportedly also lower than that of OPC (Engel'sht and Muratalieva, 2013). Furthermore, non-hydraulic CSCs are solidified by carbonation reaction, indicating that the curing inevitably sequestrates the CO_2 in the matrix via carbon mineralization. The type of cement can reduce CO_2 emission by more than 30 % compared to the OPC (Wang et al., 2022). Despite the environmental advantages, the type of cements has various technical drawbacks due to its non-hydraulic characteristics. Thus, studies on multi-component cements including hydraulic cements should be conducted to secure the early strength of CSCs.

The effects of pre-curing periods on the physical characteristics of OPC pastes with CSC in the present study were investigated to provide the knowledge of the microstructural evolution of the pastes due to pre-curing periods. The Independent variable is the pre-curing period. The pre-curing period varied from 0 to 5 hrs, considering the hydration characteristics of OPC. The carbonation curing of the OPC pastes with CSC after pre-curing was conducted. The concentration of gaseous CO_2 was fixed at 20 %.

2. Experimental Procedure

2.1 Raw materials

Calcium silicate cement (CSC) and ordinary Portland cement (OPC, HANIL Cement Co. Ltd., in Korea) were used as binder materials. The molar ratio of Ca and Si for the synthesis of CSC clinker was fixed at 1:1 based on the XRF results of starting materials. The Ca and Si components were provided with limestones and silica fume, respectively. The incineration temperature and period for the synthesis of CSC clinker were approximately 1200 °C and 4 hrs, respectively.

The chemical compositions of the OPC and the CSC used in the present study were listed in Table 1. The CSC dominantly consisted of CaO and SiO_2. The compositions of CaO and SiO_2 in the CSC were more than 90 %, while that of CaO and SiO_2 in the OPC was approximately 80 %. Instead, the OPC contained other components such as Al_2O_3, MgO, and Fe_2O_3. Figure 1 showed the XRD patterns of CSC and OPC. The patterns of CSC showed the peaks corresponding to the presence of rankinite (C_3S_2), pseudo wollastonite (CS), portlandite ($Ca(OH)_2$), cristobalite (SiO_2), lime (CaO), aragonite ($CaCO_3$), calcite ($CaCO_3$), γ-C_2S. The pseudo wollastonite(CS), and rankinite (C_3S_2) capable of reacting with CO_2 are typical phases in CSCs. The patterns of OPC showed the typical peaks corresponding to the presence of Alite (C_3S), tricalcium aluminate C_3A, brownmillerite (C_4AF), gypsum, and Larnite (β-C_2S).

Table 1. Chemical composition of OPC and CSC powders

Components	Composition (%)	
	OPC	CSC
CaO	60.3	51.6
SiO_2	20.4	46
Al_2O_3	4.6	0.38
TiO_2	0.3	0.12
Na_2O	0.2	-
MgO	3.3	0.45
Fe_2O_3	3.2	0.75
SO_3	2.3	-

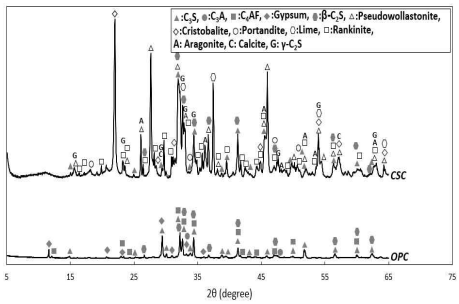

Fig. 1. XRD patterns of OPC and CSC powders:

Figure 2 showed the particle size distribution curves of CSC and OPC measured by a laser diffraction particle size analyzer (MS3000, Malvern Instruments, UK).

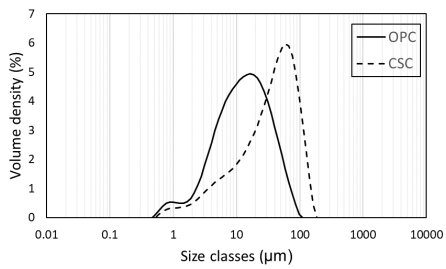

Fig. 2. Particle size distribution curves of OPC and CSC powders

The particle size of CSC powder was larger than that of OPC powder, as indicated by the shift of the CSC powder curve to the right side compared to the OPC powder curve. The D50 values for CSC and OPC powders were 40.2 μm and 13.8 μm, respectively.

2.2 Sample preparation

The OPC to CSC ratio to fabricate paste samples was fixed at 1: 0.9, and the water to cement ratio was also fixed at 0.4. The samples were prepared by mixing the dry materials for one minute, adding water, and mixing for an additional 3 minutes. The mixture was then cast into a cubic mold with dimensions of 50 mm x 50 mm x 50 mm. The samples before carbonation curing were cured for a designated period in the atmosphere. The pre-curing periods were 0 hr, 1 hr, and 5 hr. Each sample was then placed into a carbonation chamber with a temperature of 25° C and relative humidity of 60 %, while the concentration of gaseous CO_2 for carbonation curing was 20 %. After 24 hours, the samples were demolded and maintained under the same carbonation conditions for 3 days of curing.

2.3 Test methods

A compressive strength test was conducted using a universal testing machine with a 300 kN specification and a fixed crosshead speed of 0.6 mm/min, in accordance with ASTM C109. The pore characteristics of the OPC pastes with CSC were measured by conducting a mercury intrusion porosimetry test with a detection range of pores from 0.003 to 1,000 μm in diameter and a maximum intrusion pressure of 414 MPa. The surface tension and contact angle were held constant at 0.485 N/m and 130°, respectively. A TG test was conducted to quantitatively evaluate the content of hydrates and calcium carbonates. In TG tests using the MaxRes TGA manufactured by Mettler-Toledo, the heating rate was set at 10 °C/min, and N_2 gas was used to prevent sample oxidation. The samples for the MIP and TG tests were immersed in anhydrous ethanol after 3 days of curing and then placed in a vacuum chamber to stop additional hydration.

3. Results

3.1 Compressive strength

Figure 3 showed the compressive strength of the OPC pastes with CSC powder at 3 days of carbonation curing. The compressive strengths of the OPC pastes with CSC powder without pre-curing (C0), the pastes pre-cured for 1 hr (C1), and the pastes pre-cured for 5 hrs (C5) were 20.3 MPa, 18.1 MPa, and 18.8 MPa, respectively. That is, the compressive strengths of all the samples at 3 days were mostly similar.

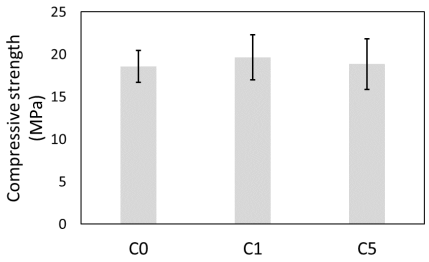

Fig 3. Compressive strength of OPC pastes with CSC powder at 3 days of curing

3.2 TG

Figure 4 showed the thermogravimetry and derivative thermogravimetry curves of OPC pastes with CSC powder pre-cured for 1 and 5 hrs. Three typical characteristic peaks in DTG curves were observed. The peaks below 200 °C occur due to the evaporation of physically and chemically bound water in the interlayers of C-S-H phases or could occur due to the decomposition of AFt and AFm phases (Seo et al., 2021). The peaks in the temperature range from 400 °C to 500 °C occur due to the decomposition of $Ca(OH)_2$, while those in the range from the 500 °C to 800 °C occur due to the decomposition of calcium carbonate phases (Seo et al., 2021; Bakolas et al., 2006). Table 2 listed the summary of weight loss obtained from thermograms of OPC pastes with CSC powder pre-cured for 1 hr and 5 hrs. The weight loss corresponding to the evaporation of physically and chemically bound water from hydrates in the C5 sample was higher than that in the C1 sample. The weight loss corresponding to the decomposition of $Ca(OH)_2$ in the C5 sample was also higher than that in the C1 sample. The weight loss relevant to calcium carbonates in the C1 sample was slightly higher than that in the C5 sample.

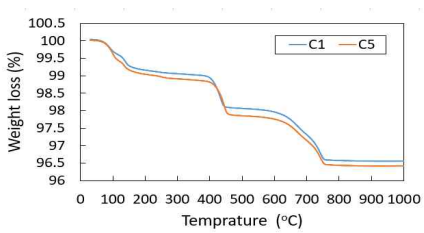

(a)

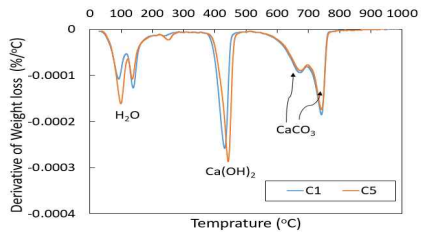

(b)

Fig 4. (a) Thermogravimetry and (b) derivative thermogravimetry curves of OPC pastes with CSC powder pre-cured for 1 and 5 hrs

Table 2. Summary of weight loss obtained from thermograms of OPC pastes with CSC powder pre-cured for 1 hr and 5 hrs

Relevant phases	Temperature (°C)	Weight loss (%)	
		C1	C5
Hydrates including C-S-H, AFt, and AFm	>200	0.84	0.95
$Ca(OH)_2$	400-500	0.95	1.01
$CaCO_3$	500-800	1.48	1.42

Figure 5 showed the thermogravimetry and derivative thermogravimetry curves of OPC pastes with CSC powder at 3 days of carbonation curing. The characteristic peaks similar to those observed in the DTG curves of the pre-cured pastes were observed. The most prominent difference is the intensity of the peaks relevant to calcium carbonates which greatly increased, while the intensity of the peaks relevant to $Ca(OH)_2$ dramatically decreased.

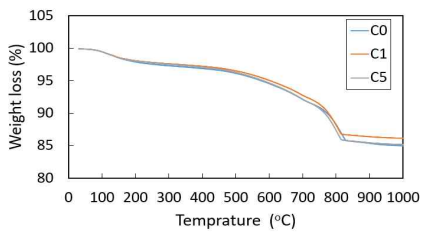

(a)

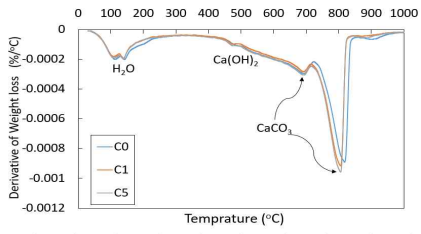

(b)

Fig 5. (a) Thermogravimetry and (b) derivative thermogravimetry curves of OPC pastes with CSC powder at 3 days of carbonation curing

Table 3 listed the summary of weight loss obtained from thermograms of OPC pastes with CSC powder at 3 days of carbonation curing. The weight loss values relevant to hydrates in the C0, C1, and C5 samples were 2.09, 1.91, and 1.95, respectively. That is, the weight loss induced by the decomposition of hydrates was highest in the C0 sample. The weight loss values relevant to the decomposition of the $Ca(OH)_2$ and calcium carbonates in the C5 sample were highest compared to those of the other samples. That is, the pre-curing period in the C5 sample slightly increased the CO_2 uptake. This is attributable that an increase in the pre-curing period promoted the formation of portlandite. The portlandite could be rapidly transformed into calcium carbonates under carbonation curing conditions.

Table 3. Summary of weight loss obtained from thermograms of OPC pastes with CSC powder at 3 days of carbonation curing

Relevant phases	Temperature (°C)	Weight loss (%)		
		C0	C1	C5
Hydrates including C-S-H, AFt, and AFm	>200	2.09	1.91	1.95
$Ca(OH)_2$	400-500	0.89	0.84	0.95
$CaCO_3$	500-800	10.54	9.97	10.63

3.3 MIP

Figure 6 showed the pore size distribution curves of OPC pastes with CSC at 3 days of carbonation curing. The test results indicated that the proportion of pores with a diameter lower than 100 nm in the C5 samples was relatively lower than those in the C0 and C1 samples. Furthermore, the proportion of pores with a diameter from 100 nm to 10,000 nm in the C5 sample was also lower than those of the C0 and C1 samples.

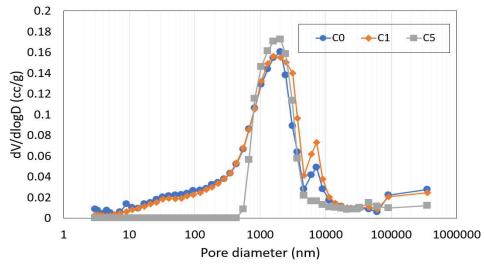

Fig 6. Pore size distribution curves of OPC pastes with CSC at 3 days of carbonation curing

4. Discussion

Typically, the heat evolution characteristics of OPCs can be divided into five zones: pre-induction, induction, acceleration, deceleration, and diffusion (Shi and Day, 1995). There are two characteristic peaks in this process. The first peak in the pre-induction zone is due to the formation of primary C-S-H phases, while the second peak between the acceleration and deceleration zone is caused by the formation of secondary C-S-H or other hydrates (Huanhai et al., 1993). The first peak finished within 1 hr, while the second peak occurred within a few hours. Meanwhile, the final setting of OPCs generally occurs between 3 hr and 7 hrs (El-Sayed et al., 2006). That is, the periods in OPCs determine the physicomechanical characteristics at an early age of curing. The pre-curing periods in the present study were 1 hr and 5 hrs to investigate the effects of the hydrates formed during pre-curing on the carbonation curing of OPC pastes with CSC.

The weight loss relevant to the hydrates of the C5 sample for the pre-curing was higher than that of the C1 sample, indicating that the amount of hydrates in the C5 sample was higher compared to that in the C1 sample. The

weight loss relevant to the portlandite of the C5 sample was also higher than that of the C1 sample. In contrast, the weight loss relevant to the hydrates and calcium carbonates of the C0 sample after carbonation curing for 3 days was slightly higher than those of other samples. Initially formed hydrates on the surface of cement particles for the pre-curing period act as a shell capable of prohibiting the dissolution of reactive components from the particles (Yi et al., 2005). That is, the initially formed hydrates on the surface of cement particles reduced the areas exposed to water. This phenomenon is called the diffusion shell effect (Yi et al., 2005). The initially formed hydrates in the C1 and C5 samples for the pre-curing period could act as a shell on the surface of cement particles, and inhibit the leaching of reactive components such as Ca and Si from OPC and CSC particles. Consequently, the weight losses relevant to hydrates and calcium carbonates of the C1 and C5 samples were relatively lower than that of the C0 sample.

In MIP test results, it was observed that the proportion of pores in the range lower than 100 nm of the C5 sample was relatively lower than those of other samples. The pores in the range of the OPC matrix generally increased as the curing period increased since the pores is formed due to the hydration reaction (Silva et al., 2001). The pores in the range from 2 nm to 10 nm are involved in the honeycomb pore structure in the C-S-H phases (Wenzel et al., 2017), and those in the range from 10 nm to 50 nm are involved in the space between interhydrates (Silva et al., 2001). The pores in the range from 0.8 nm to 80 nm in the CSC matrix are involved in the pores between calcium carbonates (Jeong, 2020). That is, the relatively lower proportion of the pores in the range lower than 100 nm in the C5 sample well supported the TG test results after carbonation curing. In addition to the shell effect of initially formed hydrates, the reaction characteristics of calcium carbonates could affect the reduction in the pores with a diameter lower than 100 nm of the C5 sample. Calcium carbonates could be formed within microseconds, while the formation of C-S-H needed more than a few minutes (Morris et al., 2020). Besides, the size of calcium carbonates has been reportedly approximately lower than 30 nm (Lin et al., 2002; Nudelman et al., 2010). Even, Sun et al. reported that amorphous calcium carbonates with a size of 2 nm were observed (Sun et al., 2016). The shoulder peaks between 500 °C-700 °C in TG test results possibly indicated the presence of amorphous calcium carbonates (Lee et al., 2016). Some ions such as Mg and Si could positively affect the formation of amorphous calcium carbonates (Gal et al., 2010; Politi et al., 2010). For the C5 samples, the leached calcium ions may not diffuse far due to the fast formation characteristics of calcium carbonates and rapidly form calcium carbonates, possibly filling the pores between hydrates. As a result, the hydrated areas surrounding the OPC and CSC particles could be densified, inhibiting the further reaction of the C5 sample for carbonation curing. The relatively higher amount of portlandite in the C5 sample compared to that in the C0 sample can be also explicated by the densification induced by the combination of hydrates and calcium carbonates surrounding OPC and CSC particles. That is, the densification may have blocked some of the pores, thereby providing a favorable condition for maintaining the portlandite phases.

While, carbonation and hydration reactions in the C0 sample may occur simultaneously since pre-curing was not conducted. A part of Ca ions leached from OPC particles quickly reacted with carbonate ions, forming calcium carbonates immediately after carbonation curing. The formation of calcium carbonates reduced the Ca ions capable of being consumed for the formation of C-S-H phases so that Ca-modified C-S-H phases could be formed in the C0 sample. Kim reported that Ca-modified C-S-H phases were observed under carbonation curing conditions at a very early age of curing (Kim, 2022). The Ca-modified C-S-H phases have been reportedly formed by the decalcification of C-S-H phases in a cementitious matrix (Kim, 2022). The decalcification of C-S-H phases increased the proportion of large capillary pores in a cement matrix (Kim et al., 2015). The condition could be favorable for a further hydration reaction in the C0 sample. Thus, the weight loss relevant to the hydrates in the C0 sample was higher than that in the C5 sample.

The proportion of pores in the range from

100 nm to 10, 000 nm of the C5 sample was lower than those of the other samples. The proportion of the pores in the OPC matrix at an early age of curing is reduced as the hydration reaction progressed since the reaction of the reactive residues in the electrolytic pore solution steadily occurs and the formed hydrates give complexity to the pore structures (Cui and Cahyadi, 2001). While, a small amount of the pores corresponding to the range in the previous study was reportedly observed in the CSC matrix compared to the OPC matrix (Jeong, 2020). Ashraf et al. (2017) reported that the three layers surrounding CSC particles were formed. Highly polymerized silica gel was formed on the surface of CSC particles, the Ca-modified silica gel on the silica gel was then formed, and calcium carbonates were formed at the outermost part of the particles (Ashraf et al., 2017). That is, the reaction products of CSC particles could grow from the surface of the particle, thereby reducing the pores from the wall side. Jeong reported that the pores in the range lower than 80 nm and more than 10,000 nm in the CSC matrix were mainly observed (Jeong 2020). As aforementioned, shell effects in the C5 sample during carbonation curing could be reinforced so that sufficient reactive ions were not provided to the electrolytic pore solution. Thus, a further hydration reaction of reactive residue in the electrolytic pore solution of the C5 sample less occurred, compared to the other samples. Furthermore, the reaction of CSC particles could fill the pores corresponding to the range. The reaction characteristics of the C5 sample were attributable to the reduction in the proportion of the pores in the range from 100 nm to 10,000 nm.

The compressive strength of all the samples in the present study was similar. Despite the clear difference in the pore characteristics among samples, the amount of reaction products was similar. In addition, the reactivity of CSC powders in the OPC pastes during carbonation curing was not investigated in the present study. Thus, a further study is needed to systematically elucidate the compressive strength test results.

4. Concluding remarks

The effects of pre-curing periods on the physical characteristics of OPC pastes with CSC in the present study were investigated. The Independent variable is the pre-curing period. The pre-curing period varied from 0 to 5 hrs, considering the hydration characteristics of OPC. The carbonation curing of the OPC pastes with CSC after pre-curing was conducted. The concentration of gaseous CO_2 was fixed at 20 %. The main conclusion drawn in the present study was as follows.

(1) The compressive strength of all the samples after carbonation curing at 3 days was mostly similar regardless of the pre-curing period.

(2) An increase in the pre-curing period reduced the hydrates in the C5 sample after carbonation curing, while the amount of portlandite slightly increased.

(3) The proportion of the pores in the range lower than 100 nm in the C5 sample was lower than those of the other samples. The proportion of the pores in the range from 100 nm to 10,000 nm in the sample was also lower than those of the other samples.

(4) Densification of the matrix surrounding OPC and CSC particles in the C5 sample possibly occurred by the filling effects of calcium carbonates in the pores between interhydrates, while the decalcification of C-S-H phases in the C0 sample probably created the pore structures capable of diffusing gaseous CO_2 into the matrix.

It can be concluded that an increase in the pre-curing period led to a change in the microstructural characteristics of OPC pastes with CSC. The present study is expected to expand the knowledge of the microstructural evolution of OPC pastes with CSC due to pre-curing periods. However, a further study is needed to investigate effects of pre-curing induced microstructural changes on the long-term reaction of the pastes.

감사의 글

This work was supported by the Industrial Strategic technology development

program-Development of manufacturing technology of hardened cement with carbonation curing (RS-2022-00155662, Development of manufacturing and application technology of 1,000 ton/year class hardened cement with carbonation curing) funded By the Ministry of Trade, Industry & Energy (MOTIE, Korea).

REFERENCES

Buzatu, A., Dill, H. G., Buzgar, N., Damian, G., Maftei, A. E., Apopei, A. I. (2016), "Efflorescent sulfates from Baia Sprie mining area (Romania)—acid mine drainage and climatological approach." Science of the Total Environment, Vol. 542, pp. 629-641.

Ashraf, W., Olek, J., Jain, J. (2017), "Microscopic features of non-hydraulic calcium silicate cement paste and mortar." Cement and Concrete Research, Vol. 100, pp. 361-372.

Bakolas, A., Aggelakopoulou, E., Moropoulou, A., Anagnostopoulou, S. (2006), "Evaluation of pozzolanic activity and physicomechanical characteristics in metakaolin-lime pastes." Journal of Thermal Analysis and Calorimetry, Vol. 84(1), pp. 157-163.

Chen, Y., Al-Neshawy, F., Punkki, J. (2021), "Investigation on the effect of entrained air on pore structure in hardened concrete using MIP." Construction and Building Materials, Vol. 292, pp. 123441.

Cui, L., Cahyadi, J. H. (2001), "Permeability and pore structure of OPC paste." Cement and Concrete Research, Vol. 31(2), pp. 277-282.

El-Sayed, M. A., El-Samni, T. M. (2006), "Physical and chemical properties of rice straw ash and its effect on the cement paste produced from different cement types." Journal of King Saud University-Engineering Sciences, Vol. 19(1), pp. 21-29.

Engel'sht, V. S., Muratalieva, V. Z. (2013), "Thermal interaction between limestone and silica." High Temperature, Vol. 51(6), pp. 769-775.

Gal, A., Weiner, S., Addadi, L. (2010), "The stabilizing effect of silicate on biogenic and synthetic amorphous calcium carbonate." Journal of the American Chemical Society, Vol. 132(38), pp. 13208-13211.

Hasanbeigi, A., Price, L., Lin, E. (2012), "Emerging energy-efficiency and CO2 emission-reduction technologies for cement and concrete production: A technical review." Renewable and Sustainable Energy Reviews, Vol. 16(8), pp. 6220-6238.

Huanhai, Z., Xuequan, W., Zhongzi, X., Mingshu, T. (1993), "Kinetic study on hydration of alkali-activated slag." Cement and Concrete Research, Vol. 23(6), pp. 1253-1258.

Jeong, H. (2020), "The influence of pore system characteristics on absorption and freeze-thaw resistance of carbonated, low-lime calcium silicate cement (CSC) based materials." (Doctoral dissertation, Purdue University Graduate School).

Kim, G. M. (2022), "Effects of carbonation on hydration characteristics of ordinary Portland cement at pre-curing condition." Journal of Urban Science, Vol. 11, pp. 21-28.

Kim, G. M., Jang, J. G., Naeem, F., Lee, H. K. (2015), "Heavy metal leaching, CO 2 uptake and mechanical characteristics of carbonated porous concrete with alkali-activated slag and bottom ash." International Journal of Concrete Structures and Materials, Vol. 9, pp. 283-294.

Lee, S. W., Kim, Y. J., Lee, Y. H., Guim, H., Han, S. M. (2016), "Behavior and characteristics of amorphous calcium carbonate and calcite using CaCO3 film synthesis." Materials & Design, Vol. 112, pp. 367-373.

Lin, R. Y., Zhang, J. Y., Zhang, P. X. (2002), "Nucleation and growth kinetics in synthesizing nanometer calcite." Journal of Crystal Growth, Vol. 245(3-4), pp. 309-320.

Morris, P. D., McPherson, I. J., Meloni, G. N., Unwin, P. R. (2020), "Nanoscale kinetics of amorphous calcium carbonate precipitation in H 2 O and D 2 O." Physical Chemistry Chemical Physics, Vol. 22(38), pp. 22107-22115.

Nudelman, F., Sonmezler, E., Bomans, P. H., Sommerdijk, N. A. (2010), "Stabilization of

amorphous calcium carbonate by controlling its particle size." Nanoscale, Vol. 2(11), pp. 2436-2439.

Politi, Y., Batchelor, D. R., Zaslansky, P., Chmelka, B. F., Weaver, J. C., Sagi, I., Addadi, L. (2010), "Role of magnesium ion in the stabilization of biogenic amorphous calcium carbonate: A structure? function investigation." Chemistry of Materials, Vol. 22(1), pp. 161-166.

Provis, J. L. (2018), "Alkali-activated materials." Cement and concrete research, Vol. 114, pp. 40-48.

Rahman, A., Rasul, M. G., Khan, M. M. K., Sharma, S. (2015), "Recent development on the uses of alternative fuels in cement manufacturing process." Fuel, Vol. 145, pp. 84-99.

Seo, J., Kim, S., Jang, D., Kim, H., Lee, H. K. (2021), "Internal carbonation of belite-rich Portland cement: An in-depth observation at the interaction of the belite phase with sodium bicarbonate." Journal of Building Engineering, Vol. 44, pp. 102907.

Shi, C., Day, R. L. (1995), "A calorimetric study of early hydration of alkali-slag cements." Cement and concrete Research, Vol. 25(6), pp. 1333-1346.

Silva, D. A., John, V. M., Ribeiro, J. L. D., Roman, H. R. (2001), "Pore size distribution of hydrated cement pastes modified with polymers." Cement and Concrete Research, Vol. 31(8), pp. 1177-1184.

Sun, S., Chevrier, D. M., Zhang, P., Gebauer, D., Clfen, H. (2016), "Distinct Short-Range Order Is Inherent to Small Amorphous Calcium Carbonate Clusters (< 2 nm)." Angewandte Chemie International Edition, Vol. 55(40), pp. 12206-12209.

Thomas, R. J., Maguire, M., Sorensen, A. D., Quezada, I. (2018), "Calcium sulfoaluminate cement." Concrete International, Vol. 40(4), pp. 65-69.

Walling, S. A., Provis, J. L. (2016), "Magnesia-based cements: a journey of 150 years, and cements for the future?." Chemical reviews, Vol. 116(7), pp. 4170-4204.

Wang, X., Guo, M. Z., Ling, T. C. (2022), "Review on CO2 curing of non-hydraulic calcium silicates cements: mechanism, carbonation and performance." Cement and Concrete Composites, pp. 104641.

Xu, J. H., Fleiter, T., Fan, Y., Eichhammer, W. (2014), "CO2 emissions reduction potential in China's cement industry compared to IEA's Cement Technology Roadmap up to 2050." Applied Energy, Vol. 130, pp. 592-602.

Yi, S. T., Moon, Y. H., Kim, J. K. (2005), "Long-term strength prediction of concrete with curing temperature." Cement and Concrete Research, Vol. 35(10), pp. 1961-1969.

Zhang, D., Ghouleh, Z., Shao, Y. (2017), "Review on carbonation curing of cement-based materials." Journal of CO2 Utilization, Vol. 21, pp. 119-131.